# MODAL PARAMETER TRACKING FOR SHAPE-CHANGING GEOMETRIC OBJECTS

*Cynthia Bruyns Maxwell*
University of California at Berkeley
Computer Science Department, CNMAT
Berkeley, California USA
cbruyns@cs.berkeley.edu

*David Bindel*
New York University
Courant Institute of Mathematical Sciences
New York, New York USA
dbindel@cims.nyu.edu

## ABSTRACT

For interactive sound synthesis, we would like to change the shape of a finite element model of an instrument and rapidly hear how the sound changes. Using modal synthesis methods, we would need to compute a new modal decomposition with each change in the geometry, making the analysis too slow for interactive use. However, by using modes computed for one geometry to estimate the frequencies for nearby geometries, we can hear much more quickly how changing the instrument shape changes the sound. In this paper, we describe how to estimate resonant frequencies of an instrument by combining information about the modes of two similar instruments. We also describe the balance between computational speed and accuracy of the computed resonances.

## 1. INTRODUCTION

With fast computers and modern techniques, we can synthesize realistic instrumental sounds in real time. The goal of the work we describe here is to *design* realistic instruments in real time. That is, we would like to know precisely how changing the shape of an instrument, or the materials that make up the instrument, will change the instrument's sound.

In modal synthesis, the motion of an instrument is expressed as a combination of modes, each of which oscillates independently of the others. To use modal synthesis, though, we must first compute a partial eigenvalue decomposition of the system matrices. This eigenvalue problem is relatively expensive, but we only need to compute the decomposition once for a given instrument. However, the eigenvalues and eigenvectors depend strongly on the instrument's shape. Therefore, to design new instrument shapes with standard modal analysis, we would need to recompute the modes for each new design – a prohibitively expensive step for an interactive tool. Our goal in this paper is to show how to quickly estimate the modes of a new instruments from the modes of one or more similar instruments.

This paper describes one method that can be used to predict how the eigenvalues and eigenvectors will move when the geometry changes. The method exploits properties of parameter-dependent linear systems by tracking an invariant subspace as modifications are made. Using this method, one avoids recomputing modes while still providing an accurate representation of the timbre of an object. The results show very high accuracy for moderate changes. Moreover, our algorithm runs in a modest linear time for standard finite element discretizations.

### 1.1. Mathematical preliminaries

For a system of *n* degrees-of-freedom (DOFs), the governing equations of motion are a set of *n* coupled ordinary differential equations of second order. The solution of these equations becomes complicated when the size of the system is large or when the forcing functions of the system are non-periodic. In such cases, it is convenient to express the deformation of the object as linear combinations of normal modes of the system. Such a transformation uncouples the equations of motion into a set of *n* uncoupled differential equations. In this form it is trivial to solve for the vibration of an object under various loading conditions.

Even when the motion of the object is large, or other nonlinear behaviors occur that violate the assumptions of modal superposition, the techniques presented in this paper can be used to build the basis that captures object motion [1], [2]. As such, this paper provides a general technique for approximating modal parameters as objects undergo shape change. It is used to aid in modal decomposition and is applied before excitation and modal superposition are performed.

The canonical system of equations resulting from discretization using the finite element method is as follows:

$$M\ddot{u} + C\dot{u} + Ku \quad = \quad f(t) \tag{1}$$

where $M$ is the matrix representing the distribution of mass in the system, $C$ is a measure of damping and $K$ is the stiffness matrix. This equation expresses the balance of forces generated by the acceleration, velocity and displacement of the object. In this form the equations are coupled and thus the solution involves manipulation of these large system matrices.

Alternatively, modal analysis seeks to decouple this system into single degree-of-freedom (DOF) oscillators. Without damping, the procedure for uncoupling these equations is straight forward using the general eigenvalue decomposition $Kx = \lambda Mx$. However, with damping, decoupling these equations requires some assumptions to be made [**?**]. Normally proportional damping is assumed such that:

$$C = \alpha_1 M + \alpha_2 K \tag{2}$$

Substituting this expression back into Equation 1, we have:

$$M(\ddot{u} + \alpha_1\dot{u}) + K(\alpha_2\dot{u} + u) \quad = \quad f(t) \tag{3}$$

This is the general form of the system before eigendecomposition.

### 1.2. Model reduction

The eigenvalue problem that we want to solve then is:

$$Ax = \lambda Bx \tag{4}$$

where $A$ and $B$ are the positive semi-definite symmetric stiffness and mass matrices respectively (i.e. $K$ and $M$), and $x$ is the vector of nodal displacements of the mode with natural frequency $\lambda = \omega^2$. One means of formulating approximate equations for freely vibrating discrete systems is via the Rayleigh's quotient:

$$\lambda_R = \frac{\hat{x}^T A \hat{x}}{\hat{x}^T B \hat{x}} \tag{5}$$

where $\hat{x}$ is an approximation to $x$ [4]. The relative accuracy of methods based upon this formulation results from the fact that eigenvalues $\lambda$ are stationary with respect to perturbations in the elements of $A, B$, and the eigenvectors $x$. Thus, if a transformation for the $n$ physical node displacements, $\hat{x}$, into fewer $(m < n)$ generalized coordinates is available, say

$$\underset{n \times 1}{\hat{x}} = \underset{n \times m}{V} \underset{m \times 1}{y} \tag{6}$$

then the corresponding Rayleigh quotient becomes

$$\lambda_R = \frac{y^T V^T A V y}{y^T V^T B V y}. \tag{7}$$

Making $\lambda_R$ stationary to arbitrary variations in the $m$ elements of $y$ yields the reduced eigenproblem

$$V^T A V y = \lambda_R V^T B V y. \tag{8}$$

We can view this reduction as imposing $n - m$ constraints on the original system thus giving the following result using the Cauchy Interlace Theorem

$$\lambda^{(i)} \leq \lambda_R^{(i)} \leq \lambda^{(j+n-m)} \;\; j \leq m. \tag{9}$$

Thus all the $\lambda_R$ are contained between $\lambda^{(i)}$ and $\lambda^{(n)}$ and the approximations become exact for $m = n$.

The essence of the reduction scheme lies in the definition of the transformation matrix $V$. Some researchers have used matrices comprised from vectors that span a Krylov subspace [5], [4]; we choose to use a matrix that is made from exact modal vectors [6].

## 2. METHODS

For most systems, only the first few natural frequencies and associated natural modes greatly influence the dynamic response, and the contribution of higher natural frequencies and the corresponding mode shapes is negligible. If only the fundamental natural frequency of the system is required, the Rayleigh method can be used. However, if a *small number* of lowest natural frequencies of the system is required, the Rayleigh-Ritz method can be used.

The Rayleigh-Ritz method then, can be considered an extension of the Rayleigh method [7]. In the Rayleigh-Ritz method, the shape of deformation of the continuous system, $v(x)$ is approximated using a trial family of admissible functions that satisfy some geometric boundary condition of the problem:

$$v(x) = \sum_{i=1}^{n} c_i \phi_i(x) \tag{10}$$

where $c_i$ are unknown constant coefficients and $\phi_i$ are the known trial family of admissible functions. The functions can be a set of assumed mode shapes, polynomials, or eigenfunctions.

The accuracy of the method depends on the value of $n$ and the choice of trial functions $\phi_i(x)$ used in the approximation. By using a larger $n$, the approximation can be made more accurate, and by using trial functions which are close to the true eigenfunctions, the approximation can be improved.

### 2.1. Approximations from a subspace

Let $s$ denote a geometric parameter. For a given finite element model, we have a generalized eigenvalue problem:

$$(K(s) - \lambda(s) * M(s))u(s) = 0, \tag{11}$$

where $K(s)$ is the stiffness matrix of the system and $M(s)$ is the mass matrix at the given state of the geometry, and $\lambda(s)$ and $u(s)$ are an eigenvalue and its corresponding eigenvector for the system.

If $w(s)$ is accurate to $O(h)$ as an estimate for $u(s)$, then

$$\mu(s) = (w(s)^* K(s) w(s))/(w(s)^* M(s) w(s)) \tag{12}$$

is accurate to $O(h^2)$ as an estimate for $\lambda(s)$. This is the accuracy boost we want to utilize.

Suppose that we have computed eigenpairs $(\lambda(s_0), u(s_0))$ and $(\lambda(s_1), u(s_1))$, and now want to compute the pair $(\lambda(s_2), u(s_2))$. Then we can use the initial approximation $\mu(s)$ drawn from a Rayleigh-Ritz approximation on the pencil:

$$(U^* K(s_2) U, U^* M(s_2) U) \tag{13}$$

where $U = [u(s_0), u(s_1)]$ (or if several of the lowest eigenvalues are desired then simply replace $u(s_0)$ with $u1(s_0), u2(s_0)$, ... and $u(s_1)$ with $u1(s_1), u2(s_1)$, etc.).

If the step size is $O(h)$, then the error in approximating $u_i(s_2)$ by extrapolating through $u_i(s_0)$ and $u_i(s_1)$ should be $O(h^2)$ – the approximation is good through the linear term – and the eigenvalue approximation should be $O(h^4)$. More generally, if you use invariant subspaces computed at $k$ points, you should get $O(h^k)$ accuracy in the eigenvector, and a corresponding $O(h^{2k})$ accuracy in the computed eigenvalue.

Therefore, by building a basis from $n$ eigenvectors sampled at $k$ locations in parameter space, we can predict the same $n$ eigenvectors and the corresponding eigenvalues at nearby points. In essence, by looking at a couple of steps, we can capture the behavior of the eigenvectors rotating as the geometry changes and by solving a smaller eigenproblem, we can reduce the time to compute the original system in order to determine a subset of eigenvalues and eigenvectors.

### 2.2. Expected behavior

Instead of solving the entire eigenvalue problem, we will be making approximations to the solutions by projecting onto the subspaces formed by analyzing nearby shapes. We can measure how well our method approximates the true eigenvectors of the system by measuring the angle between the actual and approximated eigenvectors [8], [6], [9]. One can approximate the angle by:

$$\| \sin \psi \| \leq \frac{\|r(y)\|}{gap(\theta)} \tag{14}$$

where $\theta = y^* A y$ is the Rayleigh quotient given by projection of the matrix $A$ onto the vector $y$. The residual $r(y) = Ay - y\theta$ measures how well the vector $y$ approximates an eigenvector. Also

the $gap(\theta) = min|\lambda_i[A] - \theta|$ over all $\lambda_i \neq \alpha_i$ measures how well-separated a given eigenvalue is. This result combines several important facts. Firstly, it says that the larger the gap between an eigenvalue and the neighboring eigenvalues in the same spectrum, the better the approximation one can make to its eigenvector. The next fact is more straightforward; it states that the better the vector $y$ acts like a solution to the eigenproblem $Ax - \lambda x = 0$, the better it approximates an eigenvector. From these results we know that systems with repeated or tightly clustered eigenvalues will be a problem, and we will give an example on the effect of approximation techniques on these systems in Section 3.2. However, for general parameter dependent matrices, we can see that approximation using projections onto a subspace show promise.

We will try the Rayleigh-Ritz technique on several examples to see how well we can approximate the spectrum after modifications to the geometry.

## 3. RESULTS

We tested the usefulness of this approach on a variety of experiments. The geometries tested do not represent full instruments per-se, but instead are arbitrary shapes that can be formed using the parametric method described in [10]. We use these shapes for examination of the method.

For each geometry, we used a linear shell finite element formulation as described in [11]. Each element consists of four nodes each with six degrees-of-freedom. We use shells to make the axisymmetric example easier to visualize. However this method can be used with any geometric discretization that can be defined parametrically, including solid models.

### 3.1. Separated spectrum

First, we examined a shell whose curvature is defined by four control points as shown in Figure 1. The large dots indicate the points modified directly and the smaller dots represent the points which are interpolated using cubic B-spline interpolation to define the curve. By changing the location of these control points, we change the geometry parametrically.

The control points define a curve which is then revolved by a small amount around the $z$-axis to form the geometry shown in Figure 2. We use this geometry to highlight one aspect of the method that occurs when the curve is revolved all the way around the $z$-axis.

We examined changing a 1m tall by 0.5m radius shell's outermost radius by 10cm, 1cm, and 1mm and examined the error in eigendecomposition. We considered using only one sample point in parameter space, $s$, and examined the accuracy in prediction of the Ritz values. The results show prediction errors of 1% for the smallest step size and 100% for the largest step size. As expected, smaller changes in geometry allowed for better prediction of the new eigensolution. In each of the plots, we consider the first $n$ non-zero eigenvalues.

Next, we examined using two sample points. Figure 4 shows the results for the different step sizes. As expected, using more points in parameter space increased the accuracy of the predictions. In fact, the accuracy of the two-subspace version is almost twice as many digits as the one-subspace version which agrees with the theoretical bounds in Section 2.2.

Figure 5 shows that using two subspaces versus one also gives much faster convergence. Notice how the two point version has

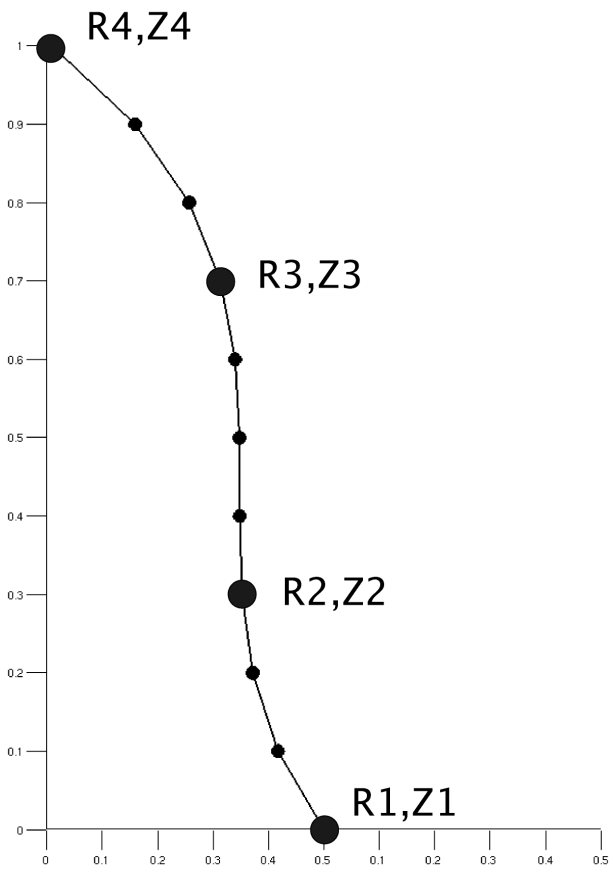


Figure 1: Parametric curve.

a steeper slope than the one point version, following the expected $O(h^{2k})$ convergence, (where $k$ is the number of points).

We also investigated using a larger subspace. So instead of using the first 50 eigenvectors, we used the first 100. Figure 6 shows how using more eigenvectors from each of the two subspaces improves the estimate of the eigenvalues.

We also confirmed that the error is proportional to the size of the object, i.e. making a 10cm change in a 1000cm object should produce smaller errors than the same absolute change to a 10cm object. By examining Figure 7, we can see when that the error is proportional to the size of the object, as expected.

### 3.2. Repeated eigenvalues and other difficulties

As we would expect for a model with a high degree of rotational symmetry, our test problem exhibits many repeated eigenvalues. For an eigenvalue with multiplicity $m$, we cannot uniquely identify $m$ mode shapes. Even for nearly-symmetric objects, the mode shapes associated with a cluster of eigenvalues can vary wildly under small perturbations. Only the $m$-dimensional invariant subspace spanned by all the shapes for the eigenvalue cluster is uniquely defined.

The sensitivity of the mode vectors does not, on its own, imply that our method will behave poorly in the presence of repeated

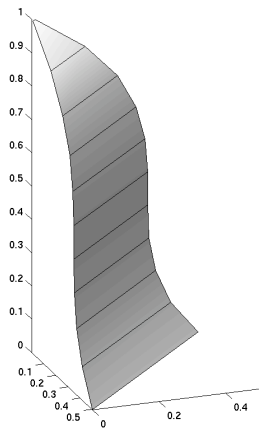

Figure 2: Simple shell model.

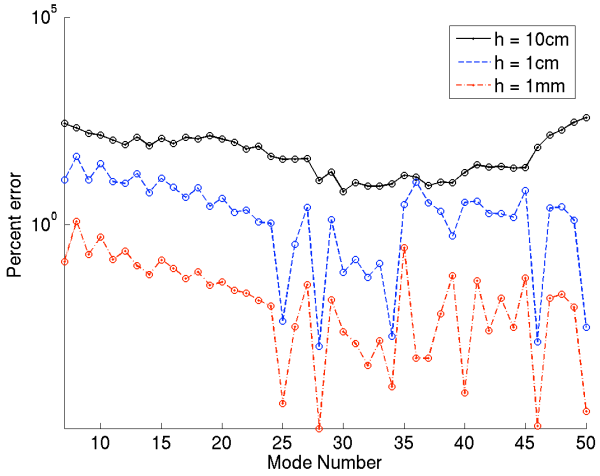


Figure 3: Error for different size $h$. One sample point.

eigenvalues. If every vector in the invariant subspace for a cluster of $m$ eigenvalues can be approximated well by some vector in the projection basis $U$, then we expect Rayleigh-Ritz approximation with $U$ to produce a cluster of $m$ eigenvalues near the original eigenvalues, and a corresponding subspace which is a good approximation to the true invariant subspace. However, the single-vector Lanczos iteration we use to find mode shapes sometimes fails to find a complete basis for each invariant subspace. When this occurs, we can overlook some of the eigenvalues and eigenvectors that we would like to capture in our projection space. When this occurs, the missing mode shapes represent a significant failure in our method.

For example, when analyzing the 1m high by 1m radius axisymmetric geometry shown in Figure 8 we found very large errors. Figure 9 shows the degeneracy that arises using a very axisymmetric geometric formulation.

We were able to resolve the some of the eigenvalues more accurately with a larger subspace, but not the eigenvalues at the beginning of the spectrum (see Figure 10).

The large errors at the beginning of the spectrum are not expected on their own, however when examining the eigenvalues we can see that the large errors can be attributed to the rapid change in eigenvectors for even a small perturbation. Figure 11 shows how the principle angles between the subspaces at two iterations can be very large for even small modifications.

In fact we found that the higher number of repeated eigenvalues, the worse the overall approximations. Figure 12 shows a geometry similar to Figure 8 but with 4 radial slices, and Figure 13 shows the error in eigenvalue approximations using this geometry. Figure 14 shows a geometry with 8 radial slices, and Figure 15 shows the error in eigenvalue approximations on this model. Figure 16 shows a geometry with 16 radial slices, and Figure 17 shows the resulting error in eigenvalue approximations. These results leads us to believe that more radial slices creates more blocks of symmetry in the system matrix, thus making it harder it is to approximate the motion of the eigenvectors.

We know two methods to address the difficulty of completely resolving the the invariant subspaces corresponding to repeated eigenvalues. The first method is to use a block version of the standard Lanczos algorithm [6]. Unlike the ordinary Lanczos iteration we use, block Lanczos iteration can find an invariant subspace for an eigenvalue in a single step, provided the block size is the same or greater than the multiplicity of the eigenvalue. The second method is the radial decomposition technique described in [10], which uses analytical knowledge of the symmetry group leading to the multiple eigenvalue in the first place.

Another source of problems is when a structure is much stiffer in some directions than in others. For example, our shell structure is much less resistant to out-of-plane bending than to in-plane compression. A vector that represents pure bending motion for one geometry may represent a mixture of bending and in-plane compression in a nearby geometry, so that a Rayleigh-Ritz approximation based on that vector will overestimate the frequency at the new geometry.

### 3.3. Performance

The speedup gained by using this method over traditional reanalysis is the difference between modest linear and super-linear computing time once the initial $k$ samples have been computed. Figure 18 shows the speedup using this method over using reanalysis for increasing resolution of the object shown in Figure 2.

## 4. CONCLUSIONS

The aim of this investigation is to determine if our tracking method method can be used to predict the changes in the frequency spectrum of an object as parametric changes are made. The results of these experiments show that for moderate changes, it is possible to avoid recomputing the eigendecompositions in order to resolve the resonant frequencies of interest.

By exploiting the properties of the system matrices, we have a bound on the errors produced using different step sizes. For an interactive design tool, this would mean that the software could alert the user when errors above a given threshold have been made and signal the need for a full reanalysis.

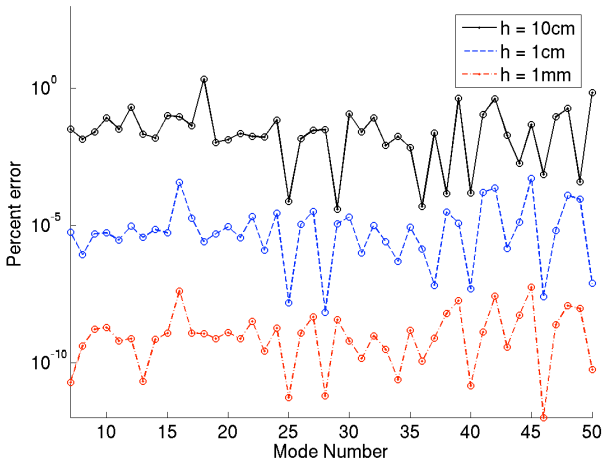


Figure 4: Error for different size $h$. Two sample points.

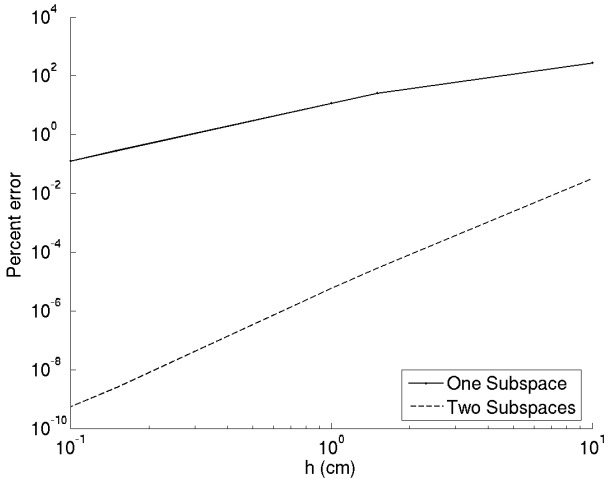


Figure 5: Error for different size $h$. Two sample points.

For systems with many repeated eigenvalues, such as axisymmetric systems, it is more beneficial to use analysis techniques that will handle the multiple eigenvalue problem.

This investigation demonstrates that for interactive design applications, it is beneficial to track the spectrum for moderate changes in geometry to avoid computing a partial eigendecomposition. By using this method, we can maintain a moderate linear time algorithm with increasing system size.

## 5. ACKNOWLEDGEMENTS

Thanks to Carlo Séquin, Antoine Chaigne and Julius O. Smith III for their comments on this work.

## 6. REFERENCES

[1] K.A. Kline, "Dynamic analysis using a reduced basis of exact modes and Ritz vectors," *AIAA Journal*, vol. 24, pp. 2022–2029, 1986.

[2] M. Lou and G. Chen, "Modal perturbation and its applications in structural systems," *Journal of Engineering Mechanics*, vol. 129, no. 8, pp. 935–943, 2003.

[3] G. B. Warburton and S. R. Soni, "Errors in response calculations for non-classically damped structures," *Earthquake Engineering & Structural Dynamics*, vol. 5, no. 4, pp. 365 – 376, 1977.

[4] I.U. Ojalvo and M. Newman, "Vibration modes of large structures by an automatic matrix-reduction method," *AIAA Journal*, vol. 8, no. 7, pp. 1234–1239, 1970.

[5] R.K. Kapania and C. Byun, "Reduction methods based on eigenvectors and Ritz vectors for nonlinear transient analysis," *Computational Mechanics*, vol. 11, pp. 65–82, 1993.

[6] B. Parlett, *The Symmetric Eigenvalue Problem (Classics in Applied Mathematics)*, SIAM, Philadelphia, 1998.

[7] S. S. Rao, *Vibration of Continuous Systems*, chapter 17, pp. 661–670, Wiley, 2007.

[8] C. Davis and W.M. Kahan, "The rotation of eigenvectors by perturbation III," *SIAM Journal of Numerical Analysis*, vol. 7, no. 1, pp. 1–46, 1970.

[9] M.E. Argentati, *Principal angles between subspaces as related to Rayleigh quotient and Rayleigh-Ritz inequalities with applications to eigenvalue accuracy and an eigenvalue solver*, Ph.D. thesis, University of Colorado at Denver, 2003.

[10] C. Bruyns and D. Bindel, "Shape-changing symmetric objects for sound synthesis," in *Proceedings AES San Francisco*, 2006.

[11] O. C. Zienkiewicz and R. L. Taylor, *Finite Element Method: Volume 2, Solid Mechanics*, Butterworth-Heinemann, Burlington, MA, 5th edition, 2000.

[12] J. W. Demmel, *Applied Numerical Linear Algebra*, SIAM, Philadelphia, 1997.

[13] R. L. Fox and M.P. Kapoor, "Rate of change of eigenvalues and eigenvectors," *AIAA Journal*, vol. 6, no. 12, pp. 2426–2429, 1968.

[14] T. Kato, *Perturbation Theory for Linear Operators*, Springer-Verlag, corrected printing of the second edition edition, 1995.

[15] Y.M. Ram, J.J. Blech, and S.G. Braun, "Eigenproblem error bounds with application to the symmetric dynamic system modification," *SIAM Journal on Matrix Analysis and Applications*, vol. 11, no. 4, pp. 553–564, 1990.

[16] Y.M. Ram and S.G. Braun, "Eigenvector error bounds and their applications to structural modifications," *AIAA Journal*, vol. 31, no. 4, pp. 759–764, 1993.

[17] Y.M. Ram, S.G. Braun, and J.J. Blech, "Structural modification in truncated systems by the Rayleigh-Ritz method," *Journal of Sound and Vibration*, vol. 125, no. 2, pp. 203–209, 1988.

[18] H.F. Weinberger, "Error bounds in the Rayleigh-Ritz approximation of eigenvectors," *Journal of Research of the National Bureau of Standards - B. Mathematics and Mathematical Physics*, vol. 64B, no. 4, pp. 217–225, 1960.

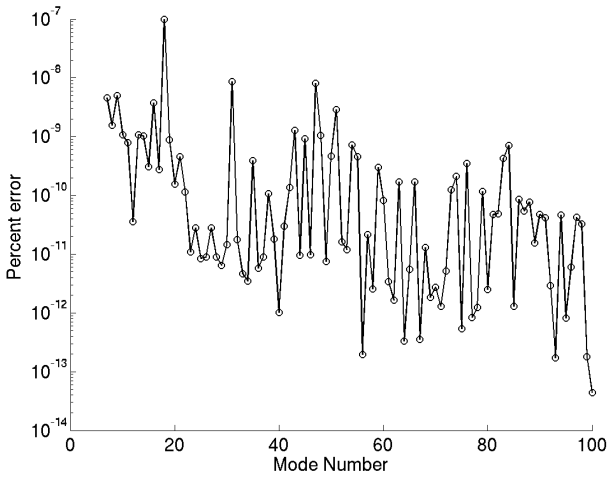


Figure 6: Error for $h = 10cm$. Larger subspaces.

[19] O. C. Zienkiewicz, J. Bauer, K. Morgan, and E. Onate, "A simple and efficient element for axisymmetric shells," *International Journal for Numerical Methods in Engineering.*, vol. 11, pp. 1545–1558, 1977.

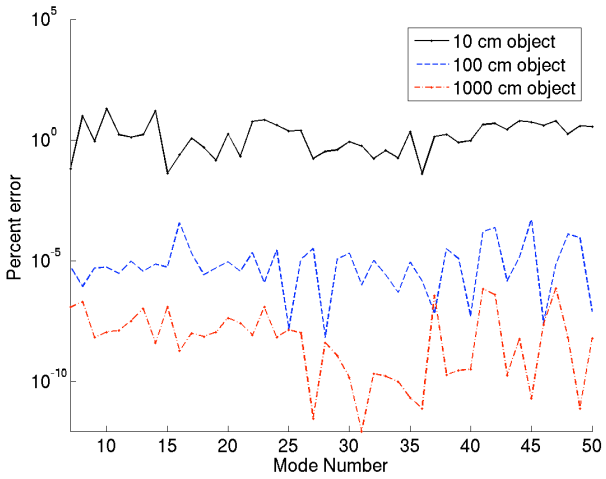


Figure 7: Error for different sized objects.

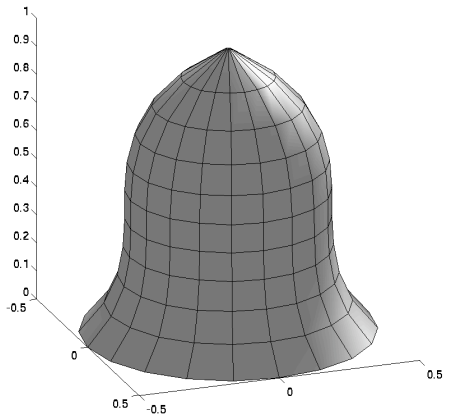

Figure 8: Axisymmetric shell model.

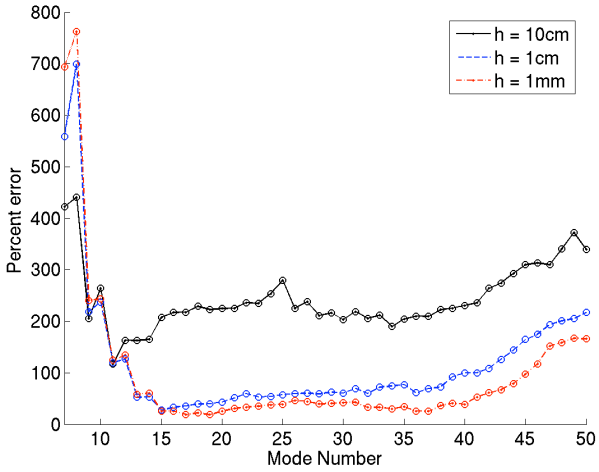


Figure 9: Error for different size $h$. Axisymmetric geometry.

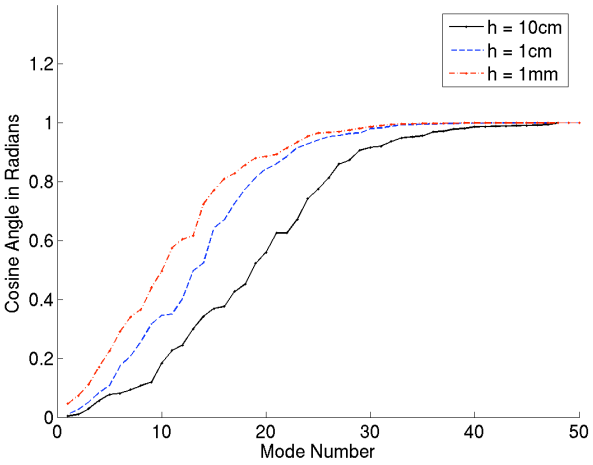


Figure 11: Cosine of angle between subspaces at two different steps.

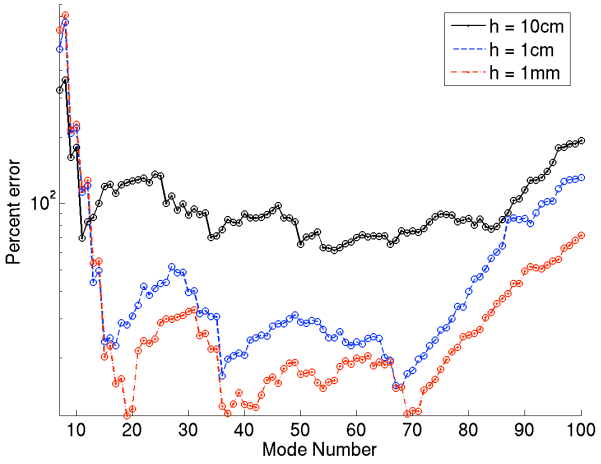


Figure 10: Error for different size $h$. Axisymmetric geometry. Larger subspace.

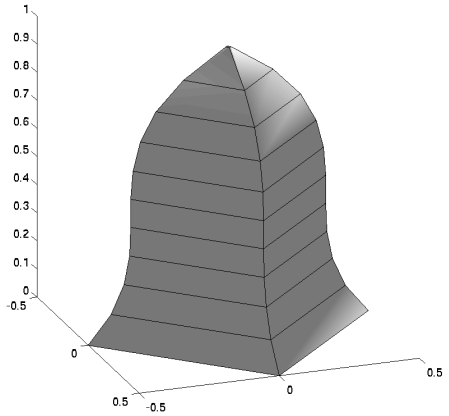

Figure 12: Whole bell geometry, 4 planes of symmetry.

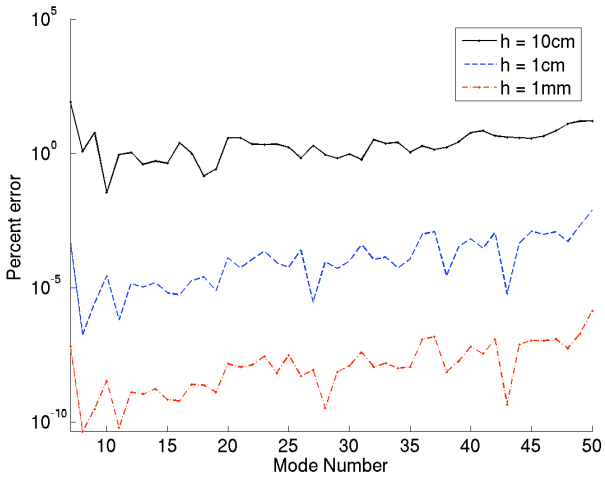


Figure 13: Error for different size $h$. 4 planes of symmetry.

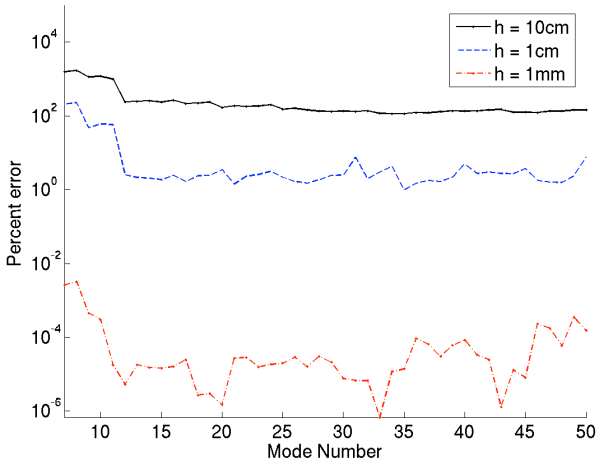


Figure 15: Error for different size $h$. 8 planes of symmetry.

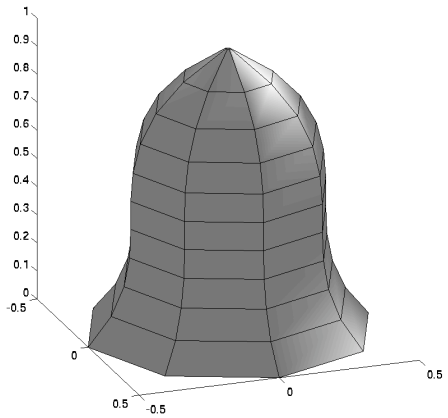

Figure 14: Whole bell geometry, 8 planes of symmetry.

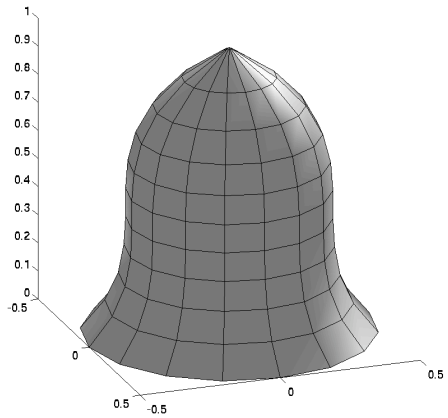

Figure 16: Whole bell geometry, 16 planes of symmetry.

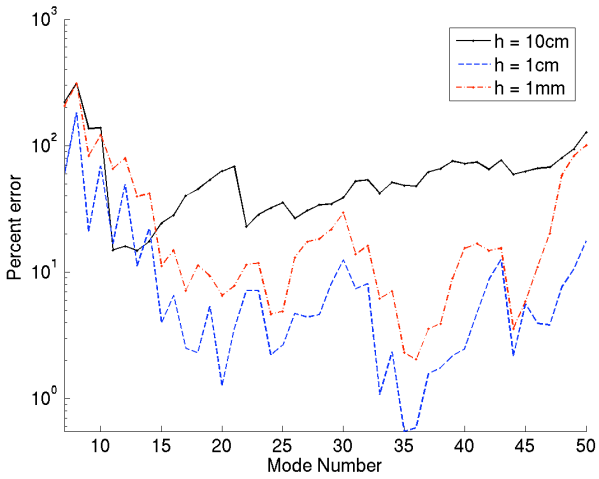


Figure 17: Error for different size $h$. 16 planes of symmetry.

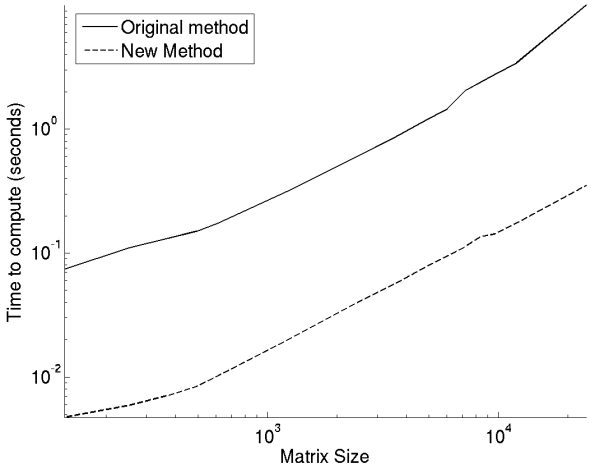


Figure 18: Time to compute new spectrum.